J Appl Electrochem (2008) 38:477–482
DOI 10.1007/s10800-007-9461-7

ORIGINAL PAPER

Electrochemical performance of chemically synthesized oligo-indole as a positive electrode for lithium rechargeable batteries

Kwang Sun Ryu · Kwang Man Kim

Received: 22 August 2007 / Revised: 13 November 2007 / Accepted: 24 November 2007 / Published online: 11 December 2007

Abstract Indole monomer was chemically polymerized to produce polyindole (PI) powder for use as a positive electrode material for lithium rechargeable batteries. Although the PI obtained was an oligomer with a low molecular weight corresponding to just 3 indole units, its electrochemical properties exhibited high d.c. electric conductivity comparable to that of the highly conducting polyaniline-$LiPF_6$ or $LiAsF_6$. A charge separation mechanism was also suggested to describe charge/discharge behavior of the oligo-indole (OI) protonated and/or lithiated in the Li||OI battery. Moreover, the lithium rechargeable battery adopting the OI as a positive electrode showed good cycleability with a discharge capacity of $\sim$55 mAh g^{-1}, which did not decay until after more than 100 cycles.

Keywords Conducting polymer · Indole · Oligo-indole · Lithium rechargeable battery

1 Introduction

Polyindole (PI) is an electroactive polymer which can demonstrate insulating and conducting properties by doping/dedoping protons or protonation/deprotonation [1, 2]. PI is also a promising material with potential applications in electrochromic devices [3], electrochemical sensors [4], and even as the electrode of rechargeable batteries [5] due to its high electrical conductivity and environmental stability in the atmosphere. The preparation of PI can be achieved by polymerization of indole monomer, C_8NH_7. Many studies involving PI have been carried out by utilizing the electropolymerization of indole [2–8] because it is easy to obtain the PI film electrodeposited on the substrate electrode, which can then be conveniently used as a test sample without modification. In the wet-process of making rechargeable battery electrodes, however, chemical polymerization of indole is required to obtain a homogeneous, highly-conducting PI powder with a high yield. Details of this chemical method are found in the journal [9–11] and patent literature [12, 13].

In the present work, indole is chemically polymerized by using an oxidizing solution of anhydrous $FeCl_3$ dissolved in chloroform. The chemically polymerized PI powder is characterized by investigating its polymer structure and molecular weight, and by examining physical properties such as morphology and thermal and crystalline properties. The PI is then electrochemically activated by a proton doping process to increase the electrical conductivity. We finally report the charge/discharge performance of a Li||PI battery after fabrication of the PI electrode and test cell to investigate the possibility of using the chemically synthesized PI powder as the cathode active material of lithium rechargeable batteries.

2 Experimental

A total of 1.44 g of indole monomer (Aldrich) was added to a mixture of 8 mL of chloroform ($CHCl_3$, Aldrich) and

K. S. Ryu (✉)
Department of Chemistry, Ulsan University, Ulsan 680-749, South Korea
e-mail: ryuks@ulsan.ac.kr

K. M. Kim (✉)
Ionics Devices Team, Electronics & Telecommunications Research Institute (ETRI), 161 Gajong, Yusong, Daejon 305-700, South Korea
e-mail: kwang@etri.re.kr

2 mL of distilled water. After the complete dissolution of indole, it was added to another solution consisting of 10 g of anhydrous $FeCl_3$ (Aldrich) dissolved in 72 mL of chloroform. The solution was then stirred for 5 h at room temperature and subsequently washed four times with distilled water, resulting in a black precipitate as a precursor of PI. The precipitate was filtered, dried in a vacuum oven for 15 h at room temperature, and finally ground with a mortar apparatus to obtain the chemically synthesized PI powder.

The PI polymerized by chemical synthesis was confirmed by molecular weight analysis using matrix-assisted laser desorption ionization mass spectroscopy (Voager® DE-STR). Some characterizations for the PI powder were also performed, such as chemical species identification before and after the polymerization using a Fourier-transform infrared spectrometer (Magna-IR 560, Nicolet) in the wavenumber range 4,000–400 cm^{-1}, morphology observation using a scanning electron microscope (Rigaku), thermal behavior analysis using a differential scanning calorimeter/thermogravimeter (SDT 2960, TA Instruments in N_2 atmosphere) in the range 25–300 °C, and crystalline properties using an X-ray diffractometer with Cu-Kα target (Rigaku) in the Bragg angle (2θ) range 5–45°.

Proton doping was carried out by impregnating PI powder into a 1 M HCl aqueous solution. Direct current (d.c.) conductivity at room temperature was measured by a standard 4-probe Van der Pauw method for the sample before and after doping. Room temperature d.c. conductivity increased from 3×10^{-4} to 1.9×10^{-3} S cm^{-1} with proton doping. We used the PI powder doped by the 1 M HCl in all subsequent characterizations. However, in order to investigate temporarily the reversibility of the doping-dedoping process, an aqueous solution containing 1 M NH_4OH was used to dedope the proton and the resultant d.c. conductivity decreased to 4.2×10^{-6} S cm^{-1} at room temperature. Redoping of the proton was carried out using the 1 M HCl aqueous solution. The d.c. conductivity recovered to 1.0×10^{-3} S cm^{-1} at room temperature, which was comparable to the value following the initial proton doping. Thus, the reversibility of the doping-dedoping process was confirmed. In addition, the temperature dependence of d.c. conductivity was also measured for the PI-HCl sample in the range 120–298 K.

A positive electrode of a test cell was composed of PI powder doped by HCl, poly(tetrafluoroethylene) binder, and carbon black conductor powder (Super P, MMM Carbon) with the weight ratio of 6:1:3, respectively. These materials were mixed in a mortar apparatus and the paste was placed on a stainless steel electrode (1 mm diameter) of a Swagelok-type electrochemical cell. Circle-shaped lithium metal foil (1 mm diameter, 80 μm thickness) was used as the negative electrode on another stainless steel electrode. The positive and negative electrodes were separated by sufficiently wetted glass-fiber filter paper as a separator, in which the electrolyte solution of 1 M $LiPF_6$ dissolved in the mixture of ethylene carbonate and dimethyl carbonate with the volume ratio of 1:1 resided. These electrodes and separator were sequentially arranged (Li||separator||PI) by using a Swagelok holder in a dry box.

The electrochemical properties of the Li||PI cell were investigated by cyclic voltammetry using a MacPile II potentiostat system at a scan rate of 1 mV s^{-1} in the potential range 1.5–4.5 V (vs. Li/Li^+). In order to examine its possibility as a rechargeable battery, the Li||PI cell was charged and discharged repeatedly using a galvanostatic charge/discharge cycler (Maccor) at a constant current of 0.1 mA and a cut-off voltage range of 2.0–4.0 V. Complex impedance spectra were also obtained using a frequency response analyzer (Solartron 1260) in the frequency range 10^{-1}–10^5 Hz after several charge/discharge cycles and after cyclic voltammetry.

3 Results and discussion

3.1 Identification of synthesized PI

Figure 1 shows the result of mass spectroscopy for the chemically synthesized PI. It can be seen that the molecular mass proceeds step by step with the molecular mass unit of indole monomer ($C_8NH_7 \cong 117$ g mol^{-1}). As a result, oligomers with 2 (indicated as 236.44 and 246.52 in Fig. 1) and 3 indole units (346.37) are likely dominantly along with minor oligomers with 5 (575.07) and 6 indole units (693.31). The oligomer with 12 indole units (1356.98), present at trace levels, was the longest chain produced. As

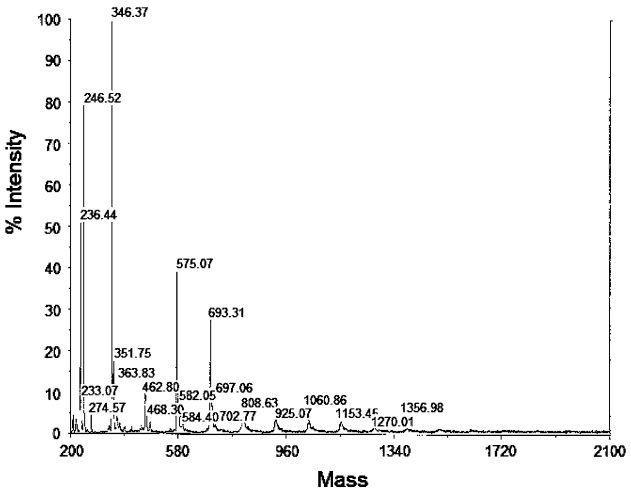

Fig. 1 Mass spectroscopy of PI chemically synthesized using $FeCl_3$ oxidant

an approximation, we estimated the number-average molecular weight M_n using a hypothesis that the percent intensity in Fig. 1 corresponds linearly to the chain length of PI. The M_n was calculated to about 348, excluding the contributions of trace oligomers which had percent intensities less than 10%. This M_n value of 348 indicates that very short chains of PI, consisting of about 3 indole units, are dominantly produced. The low molecular weight of PI is thought to be due to the less optimized chemical synthesis conditions. To produce high molecular weight PI powder, the chemical synthesis conditions should be optimized, or another chemical route must be examined. Nonetheless, it is meaningful to show the possibility of using low molecular weight PI as an electroactive material for rechargeable batteries.

Fourier-transform infrared spectra of the indole monomer and chemically synthesized oligo-indole (OI) are shown in Fig. 2. Though there seems a slight discrepancy with earlier analyses [1, 6] which measured PI samples in the doped and the dedoped states by perchlorate anion (ClO_4^-), the dedoped (neutral) state of PI is similar to the undoped state of the OI in the present study. Based on the early peak analysis for indole monomer and the dedoped state of chemically synthesized PI [1], the formation of OI can be confirmed by changes of several peaks when comparing the spectra of OI with those of indole in Fig. 2. Specifically, the vibration of the N–H band at 3,400 cm^{-1} shifts to 3,380 cm^{-1} (not shown in Fig. 2), the C=C stretching peak at 1,370 cm^{-1} appears, the peaks at 1,350, 1,277, 930 and 500 cm^{-1} weaken or disappear and finally the peak at 721 cm^{-1} disappears. Also, the appearance of bands at 1,290 and 1,540 cm^{-1} in Fig. 2 is consistent with the fact that the dedoped state of chemically synthesized OI shows typical bands corresponding to N–H vibration at the same band sites [1]. In addition, it is probable that the OI formed should have a 2,3-coupling position because of the strong out-of-plane C–H deformation band at 745 cm^{-1}, which indicates that the benzene ring was unaffected during the polymerization of indole [14, 15]. As a result, the 2,3-coupled OI with dominant 3 indole units (see Fig. 7(a)) is the main product of chemical polymerization in the present work, which is similar to the chemical structure of cyclic indole trimer [16].

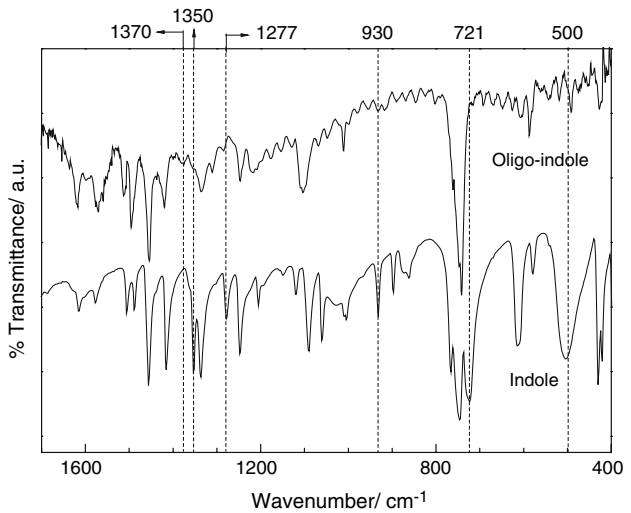

Fig. 2 Comparison of FT-IR spectra of indole monomer and chemically synthesized OI

3.2 Characteristics of OI and HCl-doped OI

Figure 3 shows a scanning electron microscopic image of chemically synthesized OI powder. Primary particles with an average diameter of 50–100 nm and aggregates of 0.1–10 μm diameter are seen to be distributed with various shapes. Chemically synthesized PI using $FeCl_3$-acetonitrile medium resulted in an average diameter of aggregates and a d.c. conductivity at room temperature somewhat lower than the other case [11] (~100 μm and 10^{-3} S cm^{-1}, respectively). Thus, the experimental synthesis condition of OI powder seems to be very important in determining the OI powder properties such as conductivity and morphology.

Figure 4 shows the thermal and crystalline properties of the OI with low molecular weight. Unlike usual conducting polymers, which generally exhibit insoluble and infusible behavior at elevated temperatures, the present OI has a low melting point at 174.8 °C with an endothermic peak and a considerable weight loss (more than 40% at 250 °C). Some temperatures of 138.5, 182.0, and 238.8 °C indicated in Fig. 4(a) are transition points of weight loss, corresponding to each structural change with increasing temperature. Broad X-ray diffraction peaks in Fig. 4(b) also show some crystallinity by polymer chain arrangement. This behavior

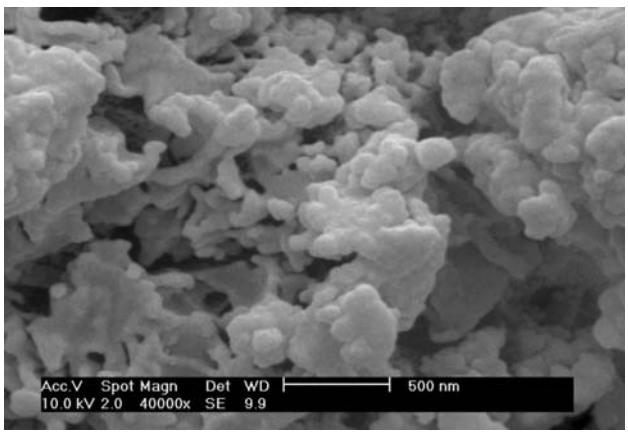

Fig. 3 Scanning electron microscopic image of chemically synthesized OI powder

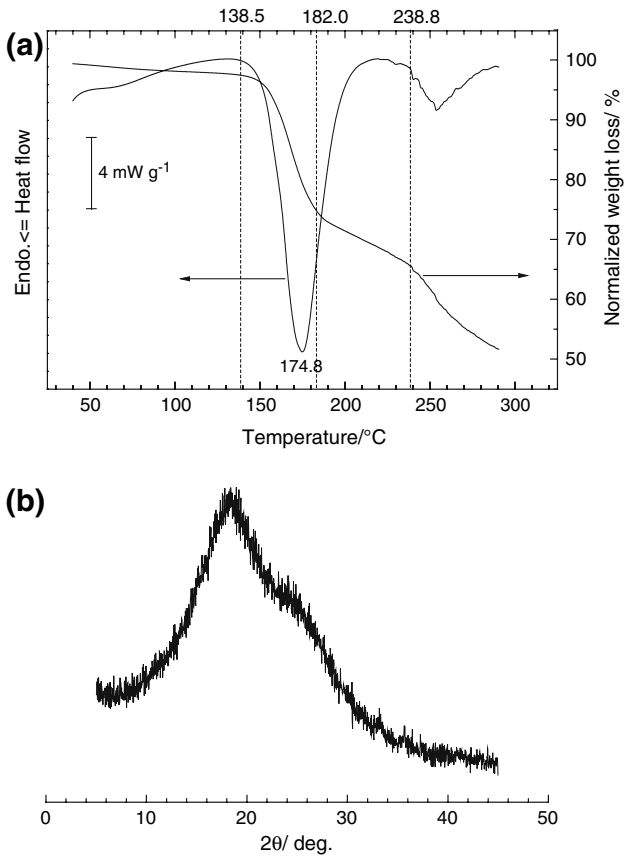

Fig. 4 (**a**) Differential scanning calorimetric thermogram and thermogravimetric results and (**b**) X-ray diffraction pattern of chemically synthesized OI

is contrary to that of PI with high molecular weight, which showed high thermal stability [4] and small weight loss of about 20% even up to 400 °C [8]. The low molecular weight of OI consisting of about 3 indole units may be the cause of the low thermal stability. The present OI, however, has the advantage of good processability at moderate temperatures, in contrast to conducting polymers with high molecular weight, which have insoluble and infusible properties leading to poor processability.

Figure 5 shows the linear dependence of d.c. conductivity $\sigma_{dc}(T)$ on the temperature T for the HCl-doped OI sample, which is plotted by a quasi-1-dimensional variable range hopping model [17] as

$$\sigma_{dc} = \sigma_0 \exp\left(-(T_0/T)^{1/2}\right)$$

where σ_0 and T_0 are constants having dimensions of conductivity and temperature, respectively. From the literature [18], the T_0 can be interpreted as an effective energy barrier or energy difference between localized states. From the slope of $\sigma_{dc}(T)$ in the plot of log σ_{dc} vs. $T^{-1/2}$, T_0 can be roughly estimated to be $\sim$15,000 K which leads to the highly conducting property of OI-HCl in comparison with the cases of polyaniline-$LiPF_6$ (T_0 = 5,400 K) and polyaniline-$LiAsF_6$ (19,000 K) [18]. The localization length can be calculated from the value of T_0 if the density of states at the Fermi level is given. As the length increases, the sample is in a relatively less localized state. The average localization length L of OI-HCl samples may be roughly approximated as 22–23 Å, similar to the previous cases of polyaniline-$LiPF_6$ (L = 23 Å) and polyaniline-$LiAsF_6$ (L = 22 Å) [18]. However, this value is probably not exact because the state density of the Fermi level is different in this type of conducting polymer.

3.3 Performance of Li||OI battery

Cyclic voltammety (CV) results in the potential range 1.5–4.5 V vs. Li/Li^+, measured using lithium salt dissolved in organic solvents for application to lithium rechargeable batteries, are shown in Fig. 6(a). This work is the first known attempt to use OI as the electrode material of lithium rechargeable batteries. Most of the previous CV studies of PI have been concentrated on the low potential region −0.5–1.2 V using standard electrodes (SHE, SCE, and Ag/AgCl) [4, 7, 14, 19]. The present OI electrode doped by HCl and mediated by 1 M $LiPF_6$ dissolved in ethylene carbonate and dimethyl carbonate (1:1 v/v), shows good reversibility in both the charging (cathodic oxidation) and discharging (anodic reduction) processes between 1.5 and 4.5 V vs. Li/Li^+.

For this charging/discharging process, the charge separation mechanism in Fig. 7(d–e) may be considered to be occurred in Li||OI batteries, in which the 2,3-coupled indole trimer in Fig. 7(a) is a main active material in the OI electrode as described above. Figure 7(b) is an example of this indole trimer in the OI-HCl electrode if fully

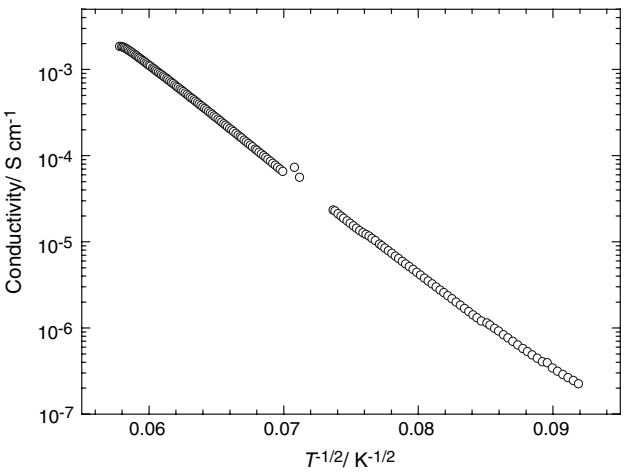

Fig. 5 Temperature dependence of d.c. conductivity for the HCl-doped OI

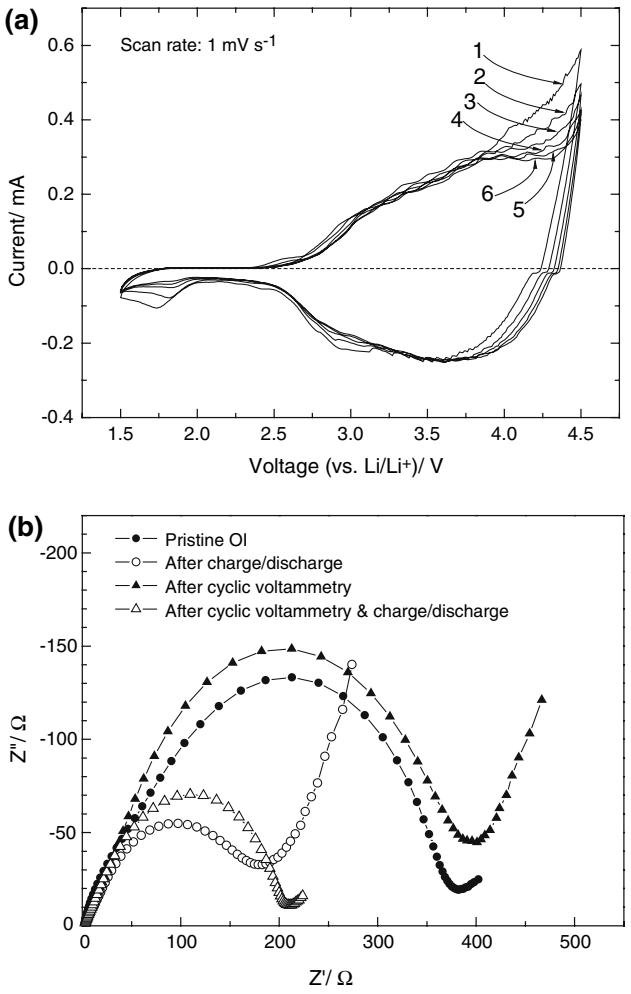

Fig. 6 (**a**) Cyclic voltammogram of the OI electrode (the numbers 1–6 are cycle numbers) and (**b**) complex impedance spectra for the OI electrode samples: pristine, after 4 cycles of charge/discharge, after 6 cycles, and after both the cyclic voltammetry and the charge/discharge

protonated, whereas Fig. 7(c) represents a fully lithiated form of the indole trimer in Li||OI batteries. It is probable that there co-exists partially protonated and/or partially lithiated indole trimers in Li||OI batteries, as shown in Fig. 7(d), in which the OI electrode is doped by HCl and simultaneously mediated by organic electrolyte containing lithium salt in the forms of dissociated cations and anions. We think that a charge separation occurs by adding PF_6^- and subtracting e^- (the charging process) to give the imine site having an unpaired electron, as shown in Fig. 7(e). It is also expected that the reverse reaction is essentially possible in the discharging process.

On the other hand, the anodic peak around 1.7 V may correspond to a small trace of lithium plating reduction on the interface between the lithium electrode and the OI electrode or separator. It is somewhat irreversible, as there is no lithium stripping oxidation peak corresponding to the lithium plating reduction. It is also uncertain, with this cyclic voltammogram, whether the OI electrode is the exact counterpart of plating lithium electrode. Here, the analysis of interfacial resistance between electrodes and/or separator, which can be calculated from the diameter of the semi-circles in the complex impedance spectra, may give information about the origin of the lithium plating reduction. As shown in Fig. 6(b), the portion of the interfacial resistance occurring during the CV repeated 6 times at the low scan rate of 1 mV s^{-1} remained constant even after subsequent charge/discharge at 0.1 mA cm^{-2}. That is, the difference (about 20 Ω) in interfacial resistance between the sample experiencing CV and the pristine sample becomes nearly equal to that between the samples experiencing [CV + charge/discharge] and undergoing charge/discharge only. The interfacial resistance of about 20 Ω occurring during the CV, irrespective of passing charge/discharge, thus originates from the irreversibility

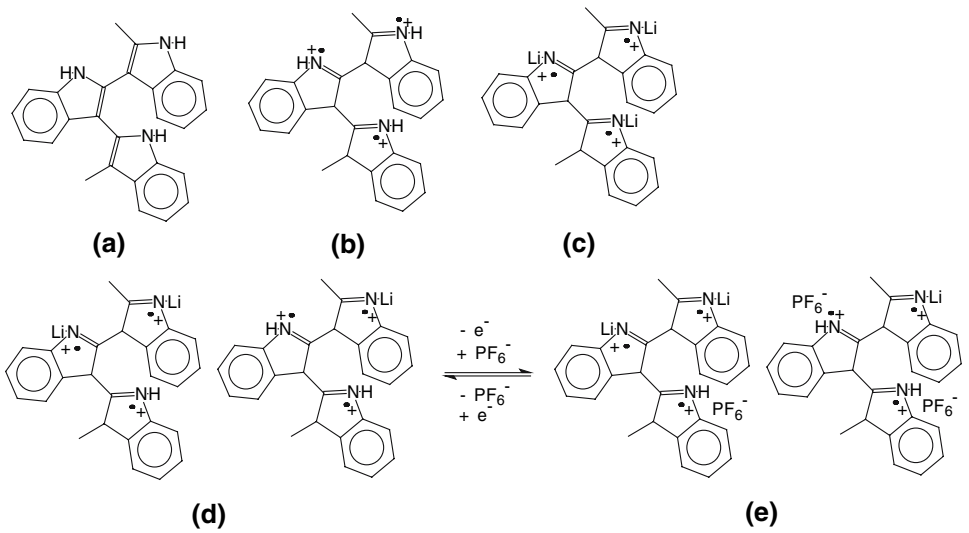

Fig. 7 Possible chemical structures and charge/discharge reaction scheme of indole trimer in Li||OI battery: (**a**) 2,3-coupled indole trimer, (**b**) fully protonated indole trimer, (**c**) fully lithiated indole trimer, (**d**) partially lithiated or protonated state (coexisted), and finally (**e**) charged state. Particularly, the (**d**) also shows the discharged state by subtracting PF_6^- and adding e^- from the (**e**)

accumulated during CV, and corresponds to the lithium plating reduction in Fig. 6(a). This minor portion of interfacial resistance during CV, compared to the dominant contribution of charge/discharge which is very reversible, may be the reason that the lithium plating first occurs on the neighboring separator, not the OI, with lithium electrode.

Figure 8 shows a typical discharge capacity profile of a Li||OI rechargeable battery in the voltage range 2.0–4.0 V. The curve is that obtained at the 20th cycle and does not exhibit a clear plateau region but has a gradual decrease in voltage up to 2.5 V. Below 2.5 V, a steep decrease in voltage occurs and thus the discharge capacity is no longer maintained. Similarly to the CV results, however, the Li||OI battery showed good reversibility (or cycleability) under repeated charge/discharge. The initial discharge capacity was greater than 70 mAh g^{-1}, but the capacity saturated at about 55 mAh g^{-1} after 50 cycles. Though the capacity of 55 mAh g^{-1} is far lower than that of using other conducting polymers as cathode material (e.g., polypyrrole-based composites [20]), the present work has a meaning that this is the first case of using electroactive indole as the active material of lithium rechargeable battery. That is to say, the present chemically synthesized OI has possible use as an electrode material in lithium rechargeable batteries. The discharge capacity of about 55 mAh g^{-1} may be confused with the result of Machida et al. [16] (55 Ah kg^{-1} = 198 F g^{-1}), which was obtained for cyclic indole trimer. However, the capacity of Machida et al. was measured in aqueous electrolyte as a capacitor, while the capacity in the present work was measured in non-aqueous organic electrolyte as a lithium rechargeable battery. In addition, higher capacity of the PI can be also expected if optimized synthesis conditions for higher molecular weight PI are established.

4 Concluding remarks

We synthesized PI power by chemical polymerization and characterized the PI for its use as the positive electrode of lithium rechargeable batteries. Although the PI obtained was an oligomer scale mostly consisting of 3 indole units, the electrochemical characterization and battery performance tests demonstrated its potential as an electrode material. In particular, the specific discharge capacity which was saturated and did not decay until more than 100 cycles had a useful value of ~55 mAh g^{-1}. Finally, it is possible to increase the discharge capacity through further optimization of synthesis conditions.

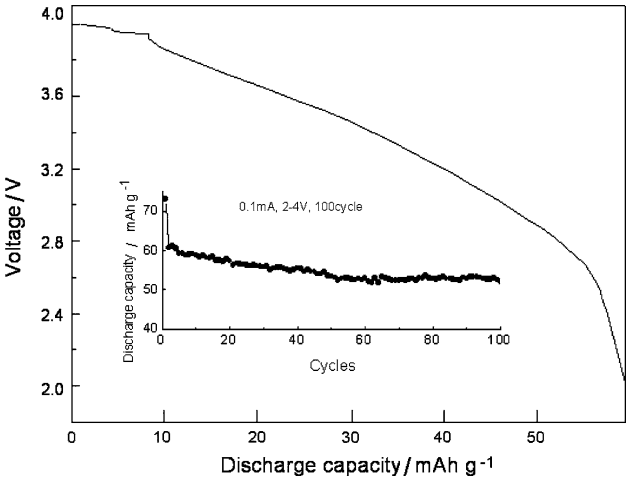

Fig. 8 Specific discharge capacity pattern of Li||OI rechargeable battery at 20th cycle. The inset shows the discharge capacity evolution of the battery over 100 cycles

Acknowledgement This work was supported by the 2007 Research Fund of University of Ulsan (Project No. 2007-0174).

References

1. Talbi H, Ghanbaja J, Billaud D, Humbert B (1997) Polymer 38:2099
2. Saraji M, Bagheri A (1998) Synth Met 98:57
3. Billaud D, Maarouf EB, Hannecart E (1994) Polymer 35:2010
4. Pandey PC, Prakash R (1998) J Electrochem Soc 145:4103
5. Pandey PC, Prakash R (1998) J Electrochem Soc 145:999
6. Talbi H, Maarouf EB, Humbert B, Alnot M, Ehrhardt JJ, Ghanbaja J, Billaud D (1996) J Phys Chem Solids 57:1145
7. Ghita M, Arrigan DWM (2004) Electroanalysis 16:979
8. Abthagir PS, Saraswathi R (2004) Thermochim Acta 424:25
9. Erlandsson R, Lundstrom I (1983) J Phys 44:713
10. Billaud D, Maarouf EM, Hannecart E (1994) Mater Res Bull 29:1239
11. Billaud D, Maarouf EB, Hannecart E (1995) Synth Met 69:571
12. Billaud D, Hannecart E, Franquist C (Solvay) (1994) US Pat 5290891
13. Kaneko S, Nishiyama T, Fujiwara M, Harada G, Kurosaki M (NEC Tokin) (2003) US Pat 6509116
14. Zotti G, Zecchin S, Schiavon G, Seraglia R, Berlin A, Canavesi A (1994) Chem Mater 6:1742
15. Xu J, Hou J, Zhou W, Nie G, Pu S, Zhang S (2006) Spectrochim Acta Part A 63:723
16. Machida K, Takenouchi H, Hiraki R, Naoi K (2005) Electrochemistry 73:489
17. Mott NF, Davis E (1979) Electronic processes in non-crystalline materials. Clarendon, Oxford
18. Jung JH, Kim BH, Moon BW, Joo J, Chang SH, Ryu KS (2001) Phys Rev B 64:035101
19. Cai Z, Geng M, Tang Z (2004) J Mater Sci 39:4001
20. Wang J, Chen J, Konstantinov K, Zhao L, Ng SH, Wang GX, Guo ZP, Liu HK (2006) Electrochim Acta 51:4634